miR-16 mimics inhibit TGF-β1-induced epithelial-to-mesenchymal transition via activation of autophagy in non-small cell lung carcinoma cells

HUI WANG, YING ZHANG, QIAN WU, YONG-BIN WANG and WEI WANG

Department of Respiratory Medicine, The Second Hospital of Shandong University, Jinan, Shandong 250033, P.R. China

Received August 16, 2017; Accepted October 30, 2017

DOI: 10.3892/or.2017.6088

Abstract. Autophagy is critical for the metastasis of cancer cells through induction of epithelial-to-mesenchymal transition (EMT). Activation of TGF-β signaling plays a key role in regulating autophagy. miR-16 may be associated with non-small cell lung carcinoma (NSCLC) progression. However, the role of miR-16 in NSCLC cell autophagy in the presence of TGF-β and the underlying mechanism are still unclear. To test whether miR-16 targets ATG3 which is involved in autophagy of NSCLC cells, we studied the expression levels of miR-16 and ATG3 in NSCLC patients, verified the targeting of ATG3 by miR-16 by luciferase reporter gene system, and investigated the role of miR-16 in the autophagy of NSCLC cells. Results revealed that miR-16 was significantly downregulated, and ATG3 was significantly upregulated in NSCLC patient tissue samples. ATG3 was found to be a direct target of miR-16. TGF-β1 significantly downregulated the expression of miR-16 and ATG3 mRNA. Using transmission electron microscopy, we observed that TGF-β1 treatment reduced autophagosomes in the A549 cells, and miR-16 mimics increased the autophagosomes in the presence of TGF-β1. Acridine orange (AO) staining and expression of LC3B II/I and p62 confirmed the inhibition of autophagy by TGF-β1, and the recovery of TGF-β1-mediated inhibition of autophagy by miR-16 mimics. Finally, miR-16 mimics inhibited TGF-β1-induced EMT, and this effect was attenuated by autophagy inhibitor 3-MA. Taken together, miR-16 mimics inhibited TGF-β1-induced EMT via activation of autophagy.

Introduction

Lung cancer is one of the most deadly malignancies, as it is the leading cause of cancer-related mortality worldwide. Lung cancer can be divided into two main subtypes: non-small cell lung cancer (NSCLC) accounting for almost 80% of lung cancer cases (1-4), and small cell lung cancer accounting for ~20% (5,6). Today, treatments for lung cancer patients rely mainly on radiotherapy and chemotherapy (7). Recent studies have shown that microRNAs (miRNAs) are of great value in the early diagnosis and treatment of NSCLC. Therefore, it is important to identify effective miRNAs and explore their roles and underlying mechanisms for the diagnosis, prediction and prevention of NSCLC (8).

miRNAs are a type of non-coding RNA (ncRNA), ~21-24 nucleotides in length, that function in the post-transcriptional regulation of gene expression. Typically miRNAs interact with specific mRNAs through complementary base-pairing to influence the translation or stability of the target mRNA molecule (9-11). The important biological processes involved in miRNAs include the development, differentiation, apoptosis and proliferation of cells (9,12,13). The abnormal expression of miRNAs is usually associated with inhibition or induction of the progression of cancer. Studies have shown that miRNAs can function as tumor-suppressor genes or oncogenes (14,15). miR-16 is widely found in different species. miR-16 plays important roles in regulating the development of organisms and cell self-renewal, differentiation and many other physiological activities. The miRNA microarray analysis of lung cancer and adjacent normal lung tissues showed the miR-16 is downregulated in lung cancer tissues (16-18). miR-16 was found to be downregulated in lung squamous cell carcinomas and adenocarcinomas, which was correlated with the expression of cyclin D1 (19). miR-16 may be a prognostic marker in NSCLC. The level of miR-16 was found to be associated with the outcome of NSCLC patients (20). Moreover, Ke *et al* demonstrated that miR-16 is downregulated in NSCLC tissue samples and cell lines (21). Overexpression of miR-16 significantly suppressed cell proliferation, colony formation, cell migration and cell invasion in NSCLC cells by targeting hepatoma-derived growth factors (21). Thus, miR-16 plays an essential role in NSCLC, and may be associated with NSCLC progression. It was reported that A549 cells express a lower level of miR-16 than normal bronchial epithelial cells, and that other mRNAs are involved in the suppression of NSCLC cell proliferation and promotion of apoptosis by miR-16 such as wip1 (17). It was reported that overexpression of miR-16 inhibited cell proliferation and induced apoptosis via regulating the expression of p27, Bcl-2, Bax and caspase-3 in NSCLC

Correspondence to: Dr Wei Wang, Department of Respiratory Medicine, The Second Hospital of Shandong University, 247 Beiyuan Street, Jinan, Shandong 250033, P.R. China
E-mail: weumwc@sina.com

Key words: miR-16, autophagy, NSCLC, TGF-β1, EMT

cells (16). A recent study demonstrated that miR-16 is a potent inducer of autophagy (22). Overexpression of miR-16 inhibited the phosphorylation of mTORC1 and p70S6K, inhibiting cell proliferation and G1/S cell cycle transition in human cervival carcinoma HeLa cells, and enhanced anticancer drug camptothecin-induced autophagy and apoptotic cell death in HeLa cells by targeting Rictor (22). Autophagy was enhanced by miR-16 overexpression in skeletal muscle (23). However, the role of miR-16 in NSCLC cell autophagy and the underlying mechanism are still unclear.

TGF-β1 plays an important role in the induction of epithelial-to-mesenchymal transition (EMT) (24,25). Other miRNAs such as miR-19 were found to inhibit the autophagy of human cardiac fibroblasts by targeting TGF-βRII mRNA during TGF-β1-induced fibrogenesis (26). Autophagy is critical for the metastasis of cancer cells through the induction of EMT and activation of TGF-β signaling plays a key role in regulating autophagy-induced EMT (27). In erlotinib-resistant lung adenocarcinoma, cells expressed high basal autophagy-related 3 protein (ATG3) (28). ATG3-mediated autophagy also plays an important role in apoptotic cell death of NSCLC cells (28).

In the present study, we hypothesized that ATG3 may be a target gene of miR-16 playing an important role in the autophagy of NSCLC cells using bioinformatics tools. To test whether miR-16 targets ATG3 which is involved in the autophagy of NSCLC cells, we studied the expression levels of miR-16 and ATG3 in NSCLC patient tissues, verified the targeting of ATG3 by miR-16 by luciferase reporter gene system, and investigated the role of miR-16 in the autophagy and EMT of NSCLC cells. Finally, the results showed that miR-16 overexpression rescued TGF-β1-mediated inhibition of autophagy and plays important roles in the EMT of NSCLC cells.

Materials and methods

NSCLC patients and tissue samples. The present study was approved by the Ethics Committee of The Second Hospital of Shandong University and was carried out according to the World Medical Association Declaration of Helsinki. All patients were enrolled after obtaining written informed consents. NSCLC tissue samples and their matched adjacent tissues were collected from 20 patients. Among these patients, 14 were male and 6 were female, with the median age of 49 years.

Cell culture and transfection. The human NSCLC cell lines A549, NCI-H1299 and HCC827 were purchased from the Cell Bank, Chinese Academy of Sciences (Shanghai, China), and the 293 cell line and normal human bronchial epithelial (HBE) cells were purchased from the American Type Culture Collection (ATCC; Manassas, VA, USA). All cells were cultured in Dulbecco's modified Eagle's medium (DMEM) containing 10% fetal bovine serum (FBS) (both from Invitrogen, Carlsbad, CA, USA) and maintained at 37˚C in a humidified atmosphere containing 5% CO_2.

Cells were treated with 5 ng/ml TGF-β1 (PeproTech, Rocky Hill, NJ, USA) for 24 h. The miR-16 mimics and negative control (NC) were purchased from Biomics Biotechnology (Jiangsu, China). A549 cells were seeded into a 6-well plate ($2.5x10^5$/well) for 24 h before transfection, and then were transfected with miR-16 mimics (50 nM) or NC (50 nM) using Lipofectamine 2000 (Invitrogen) in accordance with the manufacturer's instructions. After transfection, the cells were grown in medium without antibiotics for 48 h and then were used for the following experiments. The expression of miR-16 and ATG3 in transfected cells was detected by qRT-PCR.

Quantitative real-time polymerase chain reaction (qRT-PCR). Total RNA was extract from the tissues and cells using the RNeasy/miRNeasy kit (Qiagen, Hilden, Germany). Total RNA (1 μg) was reverse-transcribed to cDNA using SuperScript II reverse transcriptase (Invitrogen) according to the manufacturer's instructions. PCR analysis was performed using Applied Biosystems 7500 Sequence Detection system [Applied Biosystems (ABI) Foster City, CA, USA] using SYBR Premix Ex Taq GC kit (Takara, Tokyo, Japan). The following primers were used: miR-16, 5'-TCGGCGTAGCAGCACGTAAAT-3' (sense) and 5'-GTATCCAGTGCAGGGTCCGAGGT-3' (antisense); U6, 5'-CTCGCTTCGGCAGCACA-3' (sense) and 5'-AACGCTTCACGAATTTGCGT-3' (antisense); ATG3, 5'-CCAACATGGCAATGGGCTAC-3' (sense) and 5'-ACCGCCAGCATCAGTTTTGG-3' (antisense); GAPDH, 5'-CGACCACTTTGTCAAGCTCA123-3' (sense) and 5'-AGGGGAGATTCAGTGTGGTG-3' (antisense). The gene expression was normalized to the level of GAPDH using the relative ΔΔCt method.

Acridine orange (AO) staining and TEM. Formation of acidic vesicular organelles (AVO) is a characteristic feature of autophagic cells (29,30). AO staining was performed as previously described (31) to detect AVO in miR-16 mimic-transfected cells after treatment with TGF-β1. Briefly, cells grown overnight were transfected with miR-16 mimics/NC, exposed to 5 ng/ml TGF-β1 for 24 h in slide cultures, and then incubated with AO (1 μg/ml) for 15 min for staining. Another set of TGF-β1 unexposed cells was used as control. After washing thrice with phosphate-buffered saline (PBS), pH 7.4, all slides containing the AO-stained cells were detected by flow cytometric analysis (Beckman Coulter, Miami, FL, USA) after AO staining. On the basis of fluorescence intensity, formation of AVO in autophagic cells can be determined. Transmission electron microscopy (TEM) was also performed for the observation of autophagosomes. LysoTracker staining was performed by LysoTracker Red kit (Beyotime, Shanghai, China) according to the manufacturer's instructions. For detection of hydrolytic activity of cathepsin D, cells were fixed with 4% polyformaldehyde, blocked with 1% bovine serum albumin, and fixed with rabbit primary antibody (1:100; AF1645; Beyotime) overnight and incubated with the goat-anti rabbit secondary antibody (1:500; A-11034; Invitrogen). The images were captured using a confocal microscope (Leica TCS SP5; Leica Biosystems, Wetzlar, Germany).

Luciferase reporter assay and electrophoretic mobility-shift assay (EMSA). The wild-type and mutant ATG3 3'UTR sequences were amplified by PCR and ligated into the pMIR-REPORT luciferase vector (Ambion, Austin, TX, USA) to yield pMIR-ATG3 3'UTR (ATG3 3'UTR). 293 cells are easy to transfect. In the present study, we used 293T cells to detect whether miR-9 directly targets on E-cadherin. The 293 cells

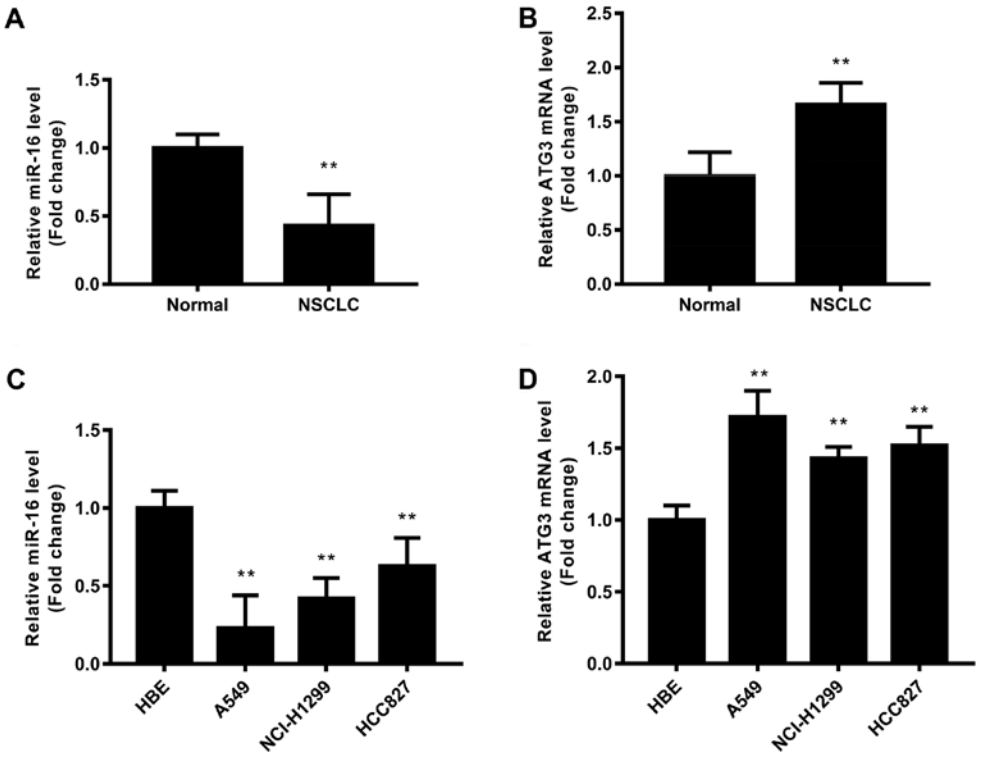

Figure 1. Expression of miR-16 and ATG3 in human NSCLC and adjacent normal tissues and cell lines. Relative expression of (A) miR-16 and (B) ATG3 was detected by qRT-PCR in NSCLC tissues and adjacent tissues; **P<0.01 vs. normal control. Relative expression of (C) miR-16, and (D) relative expression of ATG3 was detected by qRT-PCR in NSCLC cell lines; **P<0.01 vs. HBE cells.

were seeded into 6-well plates and cotransfected with wild-type/mutant ATG3 3'UTR and miR-16 mimics/NC using Lipofectamine 2000. After 24 h, cells were harvested, lysed and luciferase reporter assay was carried out according to the manufacturer's instructions (Promega, Madison, WI, USA). Interaction of miR-16 and ATG3 was detected by LightShift Chemiluminescent RNA EMSA kit (Thermo Fisher Scientific, Inc., Waltham, MA, USA) according to the manufacturer's instructions.

Western blotting. Total proteins were extracted from the NSCLC tissues and cell lines using ice-cold radioimmunoprecipitation assay (RIPA) buffer. Protein concentration was quantified using Bio-Rad DC Protein Assay kit (Bio-Rad, Hercules, CA, USA). Protein (50-100 μg) was separated on sodium dodecyl sulfate-polyacrylamide gel electrophoresis (SDS-PAGE) gel, and transferred to nitrocellulose membranes (Millipore, Billerica, MA, USA). The membranes were blocked with 5% non-fat milk in TBS-Tween and incubated with the primary antibody against ATG3 (1:500; sc-100508), LC3B (1:200; sc-271625), E-cadherin (1:200; sc-71009), V-cadherin (1:200; sc-52751) and GAPDH (1:1,000; sc-47724) overnight at 4˚C, followed by incubation with HPR-conjugated secondary antibody (all from Santa Cruz Biotechnology, Inc., Santa Cruz, CA, USA) for 60 min at room temperature. Polyclonal anti-GAPDH was used as an internal control. Then, the blots were visualized using the ECL detection system (Amersham Pharmacia Biotech, Piscataway, NJ, USA).

Cell invasion assay. Cell invasion was performed using Transwell inserts with a 8-μm membrane (Corning Inc., Corning, NY, USA) precoated with Matrigel (BD Biosciences, Franklin Lakes, NJ, USA). Cells (1x10^5/well) were seeded in the upper chamber, and medium containing 10% FBS was added to the lower chamber. Following incubation for 24 h, the non-invaded cells were removed with a swab cotton and the invaded cells on the surface of the membrane were fixed in ethanol, stained with haematoxylin, imaged and counted using microscopy.

Statistical analysis. All experiments were performed at least three times. All statistical analysis was performed using SPSS version 19.0 (SPSS, Inc., Chicago, IL, USA) using the Student's t-test. Data are presented as the mean ± SD. P<0.05 was considered to indicate a statistically significant result.

Results

miR-16 is downregulated in NSCLC tissues, and ATG3 is upregulated in NSCLC tissues. NSCLC and adjacent tissues pairs were collected (n=20), and then the expression levels of miR-16 and ATG3 mRNA were detected by qRT-PCR (Fig. 1). The results revealed that miR-16 was significantly downregulated in the NSCLC tissues compared with that noted in the normal tissues (P<0.01) (Fig. 1A). ATG3 mRNA in NSCLC tissues was significantly upregulated (P<0.01) (Fig. 1B). Thus, miR-16 was significantly downregulated and ATG3 was significantly upregulated in the NSCLC patient tissues.

In order to test the roles of miR-16 and ATG3 in NSCLC, NSCLC cell lines including A549, HCI-H1299 and HCC827 were used. The normal HBE cell line was used as a control. The results showed that miR-16 expression was significantly downregulated in all three NSCLC cell lines, while ATG3

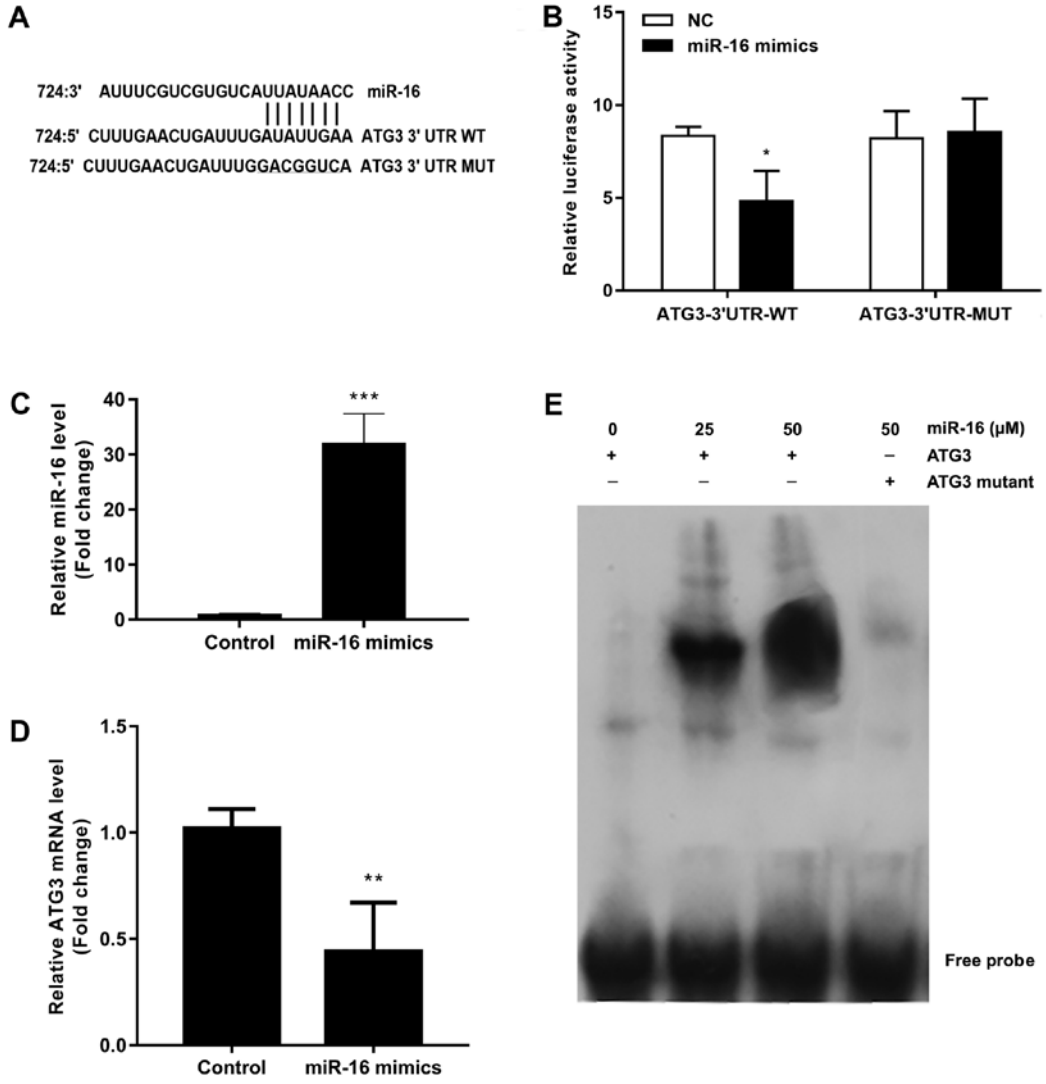

Figure 2. ATG3 is directly targeted by miR-16. (A) Bioinformatics predicted the binding site of miR-16 with ATG3 3'UTR. (B) The relative luciferase activity of ATG3 wild-type or mutant 3'UTR in 293 cells following transfection with the miR-16 mimics; *P<0.05 vs. WT or NC. (C) Relative expression of miR-16 in A549 cells transfected with miR-16 mimics. (D) Relative expression of ATG3 in A549 cells transfected with miR-16 mimics; **P<0.01, ***P<0.001 vs. control. (E) Interaction of miR-16 and ATG3 was detected by EMSA LightShift® Chemiluminescent RNA EMSA kit. Cytosolic extract of cells transfected with ATG3 wild-type (ATG3-3'UTR-WT) and ATG3-3'UTR-MUT (ATG3 mutant).

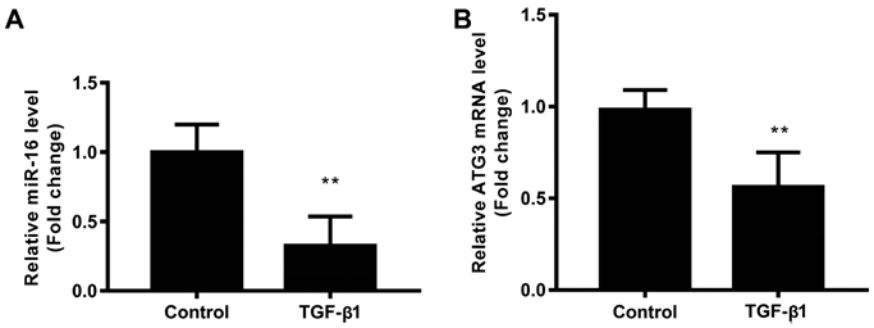

Figure 3. Expression of miR-16 and ATG3 in TGF-β1-treated NSCLC A549 cells. Relative expression of (A) miR-16 and (B) ATG3 was detected by qRT-PCR in TGF-β1-treated NSCLC A549 cells; **P<0.01 vs. the control.

mRNA was significantly upegulated in all three NSCLC cell lines, compared with the HBE cells (Fig. 1C and D). It was suggested that miR-16 expression was inversely correlated with ATG3 expression in the NSCLC cell lines. A549 that was found to have the lowest endogenous miR-16 expression and highest endogenous ATG3 expression was selected for the following experiments.

ATG3 is a direct target of miR-16. To identify whether ATG3 is a direct target gene of miR-16, we predicted the interaction

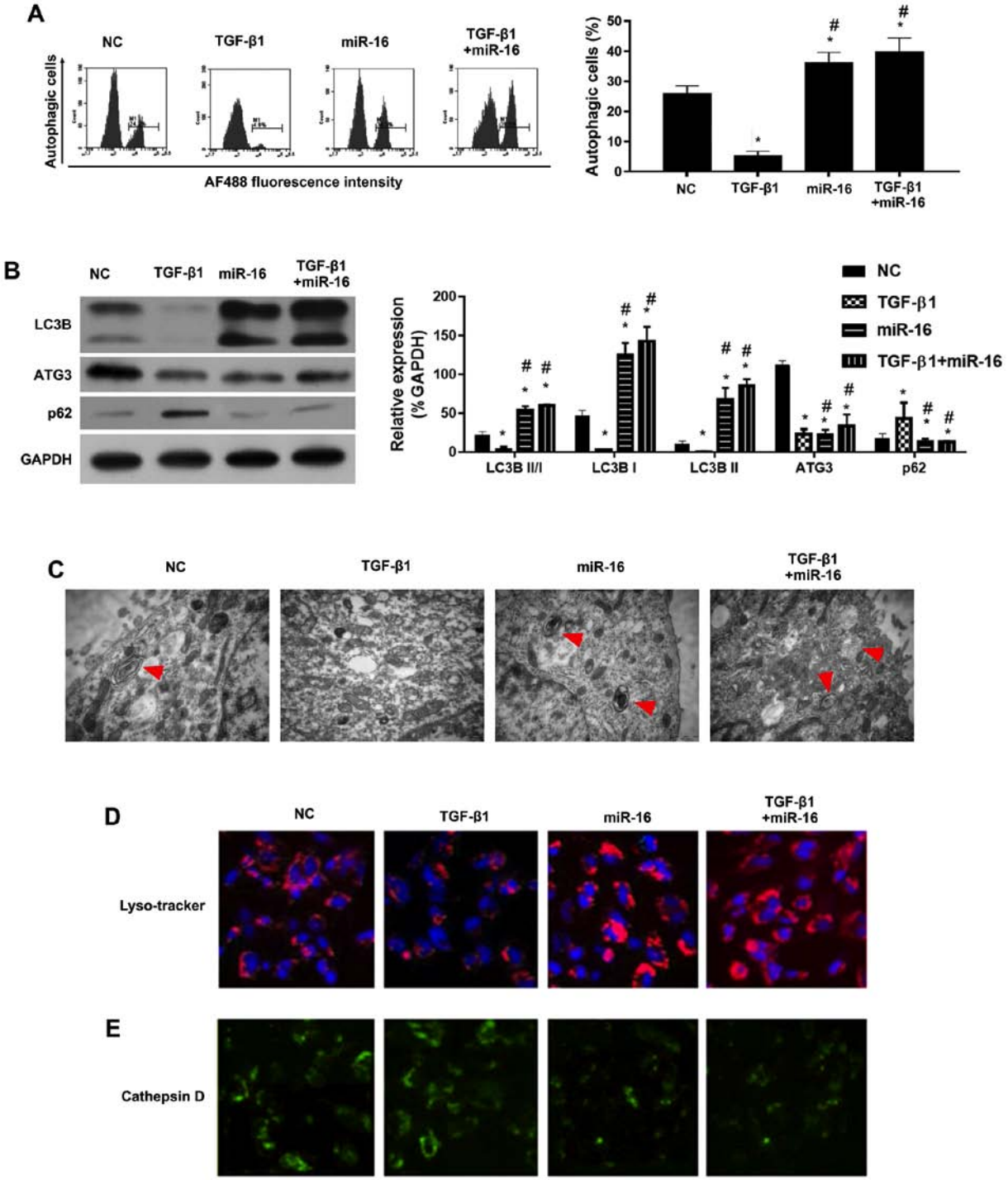

Figure 4. miR-16 mimics rescue TGF-β1-mediated inhibiiton of autophagy. After transfection with miR-16 mimics for 24 h, cells were treated with TGF-β1 (5 ng/ml) for 24 h. Then, (A) AO staining and flow cytometric analysis of autophagy was carried out. (B) Western blot analysis to evaluate the levels of autophagy-related protein LC3B. (C) TEM observation of autophagosomes. (D) LysoTracker staining. (E) Staining of cathepsin D; *P<0.05 vs. NC; #P<0.05 vs. TGF-β1. Red arrows indicate autophagosome.

site of miR-16 and ATG3 3'UTR. The predicted binding sequences of wild-type or mutant ATG3 3'UTR are shown in Fig. 2A, and they were transfected into 293 cells together with miR-16 mimics or NC. The results of the luciferase reporter assay showed that the transcriptional activity of wild-type ATG3 3'UTR was significantly decreased by miR-16 mimics (Fig. 2B). The transcriptional activity of mutant ATG3 3'URT was not affected by miR-16 mimics (Fig. 2B). The role of miR-16 in ATG3 was confirmed by transfecting miR-16 mimics into A549 cells. The results of the qRT-PCR analysis demonstrated that miR-16 was significantly upregulated in the miR-16 mimic-transfected cells (Fig. 2C), and the expression of ATG3 was also significantly downregulated in the cells transfected with the miR-16 mimics (Fig. 2D). The interaction of miR-16 and ATG3 was confirmed by EMSA (Fig. 2E).

TGF-β1 inhibits the expression of miR-16 and ATG3. To investigate the effect of miR-16 on TGF-β1-modulated NSCLC

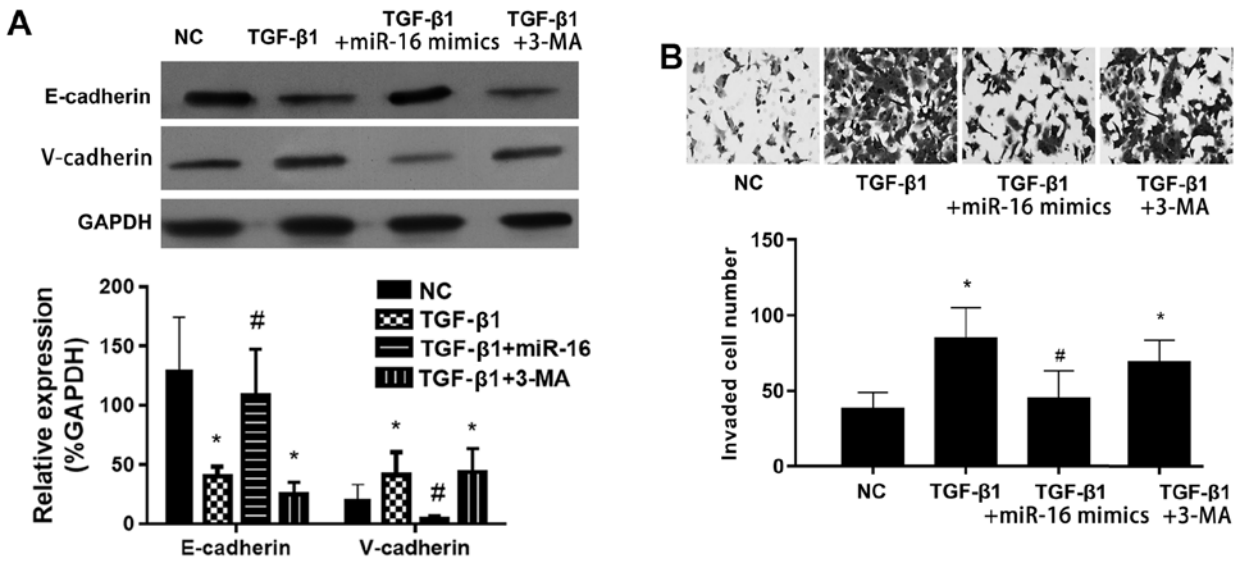

Figure 5. miR-16 mimics inhibit TGF-β1-induced EMT. After transfection with miR-16 mimics for 24 h, cells were treated with TGF-β1 (5 ng/ml) for 24 h with or without autophagy inhibitor 3-MA. Then, (A) expression levels of V-cadherin and E-cadherin were detected by western blotting. (B) Cell invasion was detected by Transwell assay; *P<0.05 vs. NC; #P<0.05 vs. TGF-β1.

cell autophagy, the expression of miR-16 and ATG3 in A549 cells in the presence of TGF-β1 were detected. Results showed that TGF-β1 significantly downregulated the expression of miR-16 (Fig. 3A), and downregulated the expression of ATG3 mRNA (Fig. 3B), indicating the miR-16 and ATG3 play an important role in TGF-β1-modulated NSCLC cell function.

miR-16 mimics rescue TGF-β1-mediated inhibition of autophagy in NSCLC cells. Recently, intense attention has been paid to the roles of autophagy in cancer development. We investigated whether TGF-β1 induced autophagy in the NSCLC cells. Cell autophagy was detected using AO staining and flow cytometry, western blotting and EMT. AO staining showed that the percentage of autophagic cells was reduced by TGF-β1 compared with the NC, and miR-16 mimics increased the percentage of autophagic cells (Fig. 4A).

Furthermore, we investigated whether there was autophagic flux in the TGF-β1 and miR-16 mimic-treated cells. As well-known and vital proteins in autophagic flux, ATG3 and LC3BI/II were detected as the representative proteins of autophagy by western blotting. Results showed a reduction in LC3BII/I levels in the TGF-β1-treated cells, and miR-16 mimics rescued the levels of LC3BII/I (Fig. 4B). TEM results confirmed the inhibition of autophagy in the presence of TGF-β1, and miR-16 enhanced autophagy in the presence of TGF-β1 (Fig. 4C).

Although ATG3 was found to be a target gene of miR-16 and ATG3 was downregulated by miR-16 mimics (Fig. 4B), miR-16 mimics increased the autophagy, indicating that ATG3 may not be involved in the TGF-β1-mediated inhibition of autophagy.

Taken together, our results indicated that miR-16 mimics rescued TGF-β1-mediated inhibition of autophagy in NSCLC cell lines. LysoTracker staining (Fig. 4D) and staining of cathepsin D (Fig. 4E) were also performed. Results showed that TGF-β1 inhibited LysoTracker staining, but the LysoTracker staining was increased following autophagic stimuli by miR-16 mimics (Fig. 4D). In contrast, cathepsin D was upregulated by TGF-β1, but was inhibited following autophagic stimuli by miR-16 mimics (Fig. 4E). There results strengthened the role of miR-16 in autophagy in the presence of TGF-β1 in NSCLC cell lines.

miR-16 mimics suppress the TGF-β1-induced EMT in NSCLC cells via activation of autophagy. miR-16 mimics reversed the TGF-β1-inhibited expression of the epithelial marker E-cadherin, while it suppressed the TGF-β1-induced expression of the mesenchymal marker V-cadherin (Fig. 5A). The effect of miR-16 mimics was inhibited by autophagy inhibitor 3-methyladenine (3-MA). The cell invasion was significantly induced by TGF-β1, and this effect was significantly inhibited by miR-16 mimics (Fig. 5B). The effect of miR-16 mimics was also inhibited by autophagy inhibitor 3-MA. These results indicated that miR-16 mimics inhibited the TGF-β1-induced EMT in NSCLC cells via activation of autophagy.

Discussion

In the present study, we detected the expression of miR-16 in NSCLC and adjacent normal tissues, predicted the binding site of ATG3 to miR-16 and confirmed the target relationship between miR-16 and ATG3 by luciferase reporter gene system. We also determined the role of miR-16 in the autophagy of NSCLC cells by transfection of miR-16 mimics into NSCLC cells.

Abnormalities in miR-16 levels have been reported in various types of cancers, suggesting that miR-16 is involved in tumor formation and progression. The miRNA microarray analysis of lung cancer and adjacent normal lung tissues showed that miR-16 was downregulated in lung cancer tissues (16-18). miR-16 plays a different role in the proliferation of different types of tumor cells by regulating a variety of mRNA target genes. For example, miR-16 was downregulated in lung squamous cell carcinomas and adenocarcinomas, which correlates

with cyclin D1 (19). miR-16 may be a prognostic marker in NSCLC. Patients with normal levels of miR-16 had the best outcome while those with high levels had the worst (20). Moreover, Ke *et al* demonstrated that miR-16 is downregulated in NSCLC tissue samples and cell lines (21). Our results revealed that miR-16 was significantly downregulated and ATG3 was significantly upregulated in patients with NSCLC.

Overexpression of miR-16 was found to significantly suppress cell proliferation and colony formation, and cell migration and invasion in NSCLC cells by targeting hepatoma-derived growth factors (21). Thus, miR-16 plays an essential role in NSCLC, and may be associated with NSCLC progression. A previous study found that A549 cells express lower level of miR-16 than normal bronchial epithelial cells, and indicated that mRNAs such as wip1 are involved in miR-16-mediated suppression of NSCLC cell proliferation and promotion of apoptosis (17). It was reported that overexpression of miR-16 inhibited cell proliferation and induced apoptosis by regulating the expression of p27, Bcl-2, Bax and caspase-3 in NSCLC cells (16). A recent study demonstrated that miR-16 is a potent inducer of autophagy (22). Overexpression of miR-16 inhibited the phosphorylation of mTORC1 and p70S6K, inhibiting cell proliferation and G1/S cell cycle transition in human cervival carcinoma HeLa cells, and enhanced anticancer drug camptothecin-induced autophagy and apoptotic cell death in HeLa cells by targeting Rictor (22). Autophagy was found to be enhanced by miR-16 overexpression in skeletal muscle (23). In the present study, we found that TGF-β1 inhibited the autophagy of NSCLC cells, and miR-16 mimics rescued the TGF-β1-mediated inhibition of autophagy.

TGF-β1 plays an important role in the induction of EMT (24,25). Other miRNAs such as miR-19 were found to inhibit the autophagy of human cardiac fibroblasts by targeting TGF-βRII mRNA during TGF-β1-induced fibrogenesis (26). Autophagy is critical for the metastasis of cancer cells through the induction of EMT and activation of TGF-β signaling plays a key role in regulating autophagy-induced EMT (27). In breast cancer, the autophagy agonist rapamycin increased TGF-β1-induced protective effects and formation of cancer-associated fibroblast phenotypes, while autophagy inhibitor 3-MA, Atg5 knockdown or TGF-β type I receptor kinase inhibitor LY-2157299 blocked TGF-β1-induced effects, indicating that TGF-β/Smad autophagy was involved in TGF-β1-induced protective effects and formation of cancer-associated fibroblast phenotype in the tumor microenvironment (32). In the present study, we found that miR-16 mimics inhibited TGF-β1-induced EMT in NSCLC cells via activation of autophagy.

Erlotinib-resistant lung adenocarcinoma cells were found to expressed high basal ATG3 (28). ATG3-mediated autophagy also plays an important role in apoptotic cell death of NSCLC cells (28). The results suggested that upregulation of ATG3 by miR-16 mimics was inhibited by TGF-β1. miR-16 mimic transfection did not further inhibit the expression of ATG3 in the presence of TGF-β1. Thus, ATG3 may not be involved in TGF-β1-mediated inhibition of autophagy. miR-16 may promote autophagy via targeting an unknown gene in the presence of TGF-β1. The molecular mechanism underlying the rescue of TGF-β1-inhibited autophagy by miR-16 warrants further study and must be confirmed using additional cell lines.

In conclusion, our results indicated that miR-16 mimics inhibited TGF-β1-induced EMT via activation of autophagy in NSCLC cell lines.

References

1. Pan X, Zhang X, Sun H, Zhang J, Yan M and Zhang H: Autophagy inhibition promotes 5-fluorouraci-induced apoptosis by stimulating ROS formation in human non-small cell lung cancer A549 cells. PLoS One 8: e56679, 2013.
2. Chiu LY, Hu ME, Yang TY, Hsin IL, Ko JL, Tsai KJ and Sheu GT: Immunomodulatory protein from *Ganoderma microsporum* induces pro-death autophagy through Akt-mTOR-p70S6K pathway inhibition in multidrug resistant lung cancer cells. PLoS One 10: e0125774, 2015.
3. Hsin IL, Sheu GT, Jan MS, Sun HL, Wu TC, Chiu LY, Lue KH and Ko JL: Inhibition of lysosome degradation on autophagosome formation and responses to GMI, an immunomodulatory protein from *Ganoderma microsporum*. Br J Pharmacol 167: 1287-1300, 2012.
4. Hsin IL, Ou CC, Wu TC, Jan MS, Wu MF, Chiu LY, Lue KH and Ko JL: GMI, an immunomodulatory protein from *Ganoderma microsporum*, induces autophagy in non-small cell lung cancer cells. Autophagy 7: 873-882, 2011.
5. Zhu L, Pickle LW, Ghosh K, Naishadham D, Portier K, Chen HS, Kim HJ, Zou Z, Cucinelli J, Kohler B, *et al*: Predicting US- and state-level cancer counts for the current calendar year: Part II: Evaluation of spatiotemporal projection methods for incidence. Cancer 118: 1100-1109, 2012.
6. Chen HS, Portier K, Ghosh K, Naishadham D, Kim HJ, Zhu L, Pickle LW, Krapcho M, Scoppa S, Jemal A, *et al*: Predicting US- and state-level cancer counts for the current calendar year: Part I: Evaluation of temporal projection methods for mortality. Cancer 118: 1091-1099, 2012.
7. Seifi-Najmi M, Hajivalili M, Safaralizadeh R, Sadreddini S, Esmaeili S, Razavi R, Ahmadi M, Mikaeili H, Baradaran B, Shams-Asenjan K, *et al*: SiRNA/DOX lodeded chitosan based nanoparticles: Development, characterization and in vitro evaluation on A549 lung cancer cell line. Cell Mol Biol 62: 87-94, 2016.
8. Li J, Yi W, Jiang P, Sun R and Li T: Effects of ambroxol hydrochloride on concentrations of paclitaxel and carboplatin in lung cancer patients at different administration times. Cell Mol Biol 62: 85-89, 2016.
9. Bartel DP: MicroRNAs: Genomics, biogenesis, mechanism, and function. Cell 116: 281-297, 2004.
10. Rajewsky N: microRNA target predictions in animals. Nat Genet 38 (Suppl 38): S8-S13, 2006.
11. Valencia-Sanchez MA, Liu J, Hannon GJ and Parker R: Control of translation and mRNA degradation by miRNAs and siRNAs. Genes Dev 20: 515-524, 2006.
12. Rosa A and Brivanlou AH: MicroRNAs in early vertebrate development. Cell Cycle 8: 3513-3520, 2009.
13. Harfe BD: MicroRNAs in vertebrate development. Curr Opin Genet Dev 15: 410-415, 2005.
14. Fattore L, Costantini S, Malpicci D, Ruggiero CF, Ascierto PA, Croce CM, Mancini R and Ciliberto G: MicroRNAs in melanoma development and resistance to target therapy. Oncotarget 8: 22262-22278, 2017.
15. Lin X, Khalid S, Qureshi MZ, Attar R, Yaylim I, Ucak I, Yaqub A, Fayyaz S, Farooqi AA and Ismail M: VEGF mediated signaling in oral cancer. Cell Mol Biol 62: 64-68, 2016.
16. Wang W, Chen J, Dai J, Zhang B, Wang F and Sun Y: MicroRNA-16-1 inhibits tumor cell proliferation and induces apoptosis in A549 non-small cell lung carcinoma cells. Oncol Res 24: 345-351, 2016.
17. Gu Y, Wang XD, Lu JJ, Lei YY, Zou JY and Luo HH: Effect of mir-16 on proliferation and apoptosis in human A549 lung adenocarcinoma cells. Int J Clin Exp Med 8: 3227-3233, 2015.
18. Fan L, Qi H, Teng J, Su B, Chen H, Wang C and Xia Q: Identification of serum miRNAs by nano-quantum dots microarray as diagnostic biomarkers for early detection of non-small cell lung cancer. Tumour Biol 37: 7777-7784, 2016.
19. Bandi N, Zbinden S, Gugger M, Arnold M, Kocher V, Hasan L, Kappeler A, Brunner T and Vassella E: miR-15a and miR-16 are implicated in cell cycle regulation in a Rb-dependent manner and are frequently deleted or down-regulated in non-small cell lung cancer. Cancer Res 69: 5553-5559, 2009.

20. Navarro A, Diaz T, Gallardo E, Viñolas N, Marrades RM, Gel B, Campayo M, Quera A, Bandres E, Garcia-Foncillas J, *et al*: Prognostic implications of miR-16 expression levels in resected non-small-cell lung cancer. J Surg Oncol 103: 411-415, 2011.
21. Ke Y, Zhao W, Xiong J and Cao R: Downregulation of miR-16 promotes growth and motility by targeting HDGF in non-small cell lung cancer cells. FEBS Lett 587: 3153-3157, 2013.
22. Huang N, Wu J, Qiu W, Lyu Q, He J, Xie W, Xu N and Zhang Y: MiR-15a and miR-16 induce autophagy and enhance chemosensitivity of camptothecin. Cancer Biol Ther 16: 941-948, 2015.
23. Lee DE, Brown JL, Rosa ME, Brown LA, Perry RA Jr, Wiggs MP, Nilsson MI, Crouse SF, Fluckey JD, Washington TA, *et al*: microRNA-16 is downregulated during insulin resistance and controls skeletal muscle protein accretion. J Cell Biochem 117: 1775-1787, 2016.
24. Zeng YE, Yao XH, Yan ZP, Liu JX and Liu XH: Potential signaling pathway involved in sphingosine-1-phosphate-induced epithelial-mesenchymal transition in cancer. Oncol Lett 12: 379-382, 2016.
25. Zeng Y, Yao X, Chen L, Yan Z, Liu J, Zhang Y, Feng T, Wu J and Liu X: Sphingosine-1-phosphate induced epithelial-mesenchymal transition of hepatocellular carcinoma via an MMP-7/ syndecan-1/TGF-β autocrine loop. Oncotarget 7: 63324-63337, 2016.
26. Zou M, Wang F, Gao R, Wu J, Ou Y, Chen X, Wang T, Zhou X, Zhu W, Li P, *et al*: Autophagy inhibition of hsa-miR-19a-3p/19b-3p by targeting TGF-β R II during TGF-β1-induced fibrogenesis in human cardiac fibroblasts. Sci Rep 6: 24747, 2016.
27. Li J, Yang B, Zhou Q, Wu Y, Shang D, Guo Y, Song Z, Zheng Q and Xiong J: Autophagy promotes hepatocellular carcinoma cell invasion through activation of epithelial-mesenchymal transition. Carcinogenesis 34: 1343-1351, 2013.
28. Lee JG and Wu R: Combination erlotinib-cisplatin and Atg3-mediated autophagy in erlotinib resistant lung cancer. PLoS One 7: e48532, 2012.
29. Guo JY and White E: Autophagy, metabolism, and cancer. Cold Spring Harb Symp Quant Biol 81: 73-78, 2016.
30. Rabinowitz JD and White E: Autophagy and metabolism. Science 330: 1344-1348, 2010.
31. Chakrabarti M, Klionsky DJ and Ray SK: miR-30e blocks autophagy and acts synergistically with proanthocyanidin for inhibition of AVEN and BIRC6 to increase apoptosis in glioblastoma stem cells and glioblastoma SNB19 cells. PLoS One 11: e0158537, 2016.
32. Liu FL, Mo EP, Yang L, Du J, Wang HS, Zhang H, Kurihara H, Xu J and Cai SH: Autophagy is involved in TGF-β1-induced protective mechanisms and formation of cancer-associated fibroblasts phenotype in tumor microenvironment. Oncotarget 7: 4122-4141, 2016.